ONCOIMMUNOLOGY
2017, VOL. 6, NO. 4, e1292195 (12 pages)
http://dx.doi.org/10.1080/2162402X.2017.1292195

Taylor & Francis
Taylor & Francis Group

ORIGINAL RESEARCH

# LYG1 exerts antitumor function through promoting the activation, proliferation, and function of CD4$^+$ T cells

Huihui Liu[a,b,*], Yanfei Zhang[a,c,*], Zhengyang Liu[a], Pingzhang Wang[a], Xiaoning Mo[a], Weiwei Fu[a], Wanchang Liu[a], Yingying Cheng[a], and Wenling Han[a]

[a]Department of Immunology, School of Basic Medical Sciences, Peking University Health Science Center, Peking University Center for Human Disease Genomics, Key Laboratory of Medical Immunology, Ministry of Health, Beijing, China; [b]Department of Hematology, Peking University First Hospital, Beijing, China; [c]Genomic Medicine Institute, Geisinger Health System, Danville, CA, USA

**ABSTRACT**

Identification of novel stimulatory cytokines with antitumor function would have great value in tumor immunotherapy investigations. Here, we report LYG1 (Lysozyme G-like 1) identified through the strategy of Immunogenomics as a novel classical secretory protein with tumor-inhibiting function. LYG1 recombinant protein (rhLYG1) could significantly suppress the growth of B16 tumors in WT B6 mice, but not in SCID-beige mice, *Rag1*$^{-/-}$ mice, CD4$^+$- or CD8$^+$ T cell-deleted mice. It could increase the number of CD4$^+$ and CD8$^+$ T cells in tumor-infiltrating lymphocytes, tumor-draining lymph nodes, and spleens, and promote IFN$\gamma$ production by T cells in tumor-bearing mice. *In vitro* experiments demonstrated that rhLYG1 could directly enhance IFN$\gamma$ secretion by CD4$^+$ T cells, but not CD8$^+$ T cells. Moreover, it could promote the activation, proliferation, and IFN$\gamma$ production of tumor antigen-specific CD4$^+$ T cells. The tumor-inhibiting effect of LYG1 was eliminated in *Ifng*$^{-/-}$ mice. Furthermore, LYG1 deficiency accelerated B16 and LLC1 tumor growth and inhibited the function of T cells. In summary, our findings reveal a tumor-inhibiting role for LYG1 through promoting the activation, proliferation, and function of CD4$^+$ T cells in antitumor immune responses, offering implications for novel tumor immunotherapy.

**Abbreviations:** CFSE, carboxyfluorescein succinimidyl ester; DC, dendritic cell; ELISA, enzyme-linked immunosorbent assay; GEWL, goose egg white lysozyme; IFN, interferon; IL, interleukin; i.p., intraperitoneally; KOMP, knock-out mouse project; LLC, Lewis lung carcinoma; LYG1, lysozyme G-like 1; NK cell, natural killer cell; OVA, ovalbumin; s.c., subcutaneously; pcDB, pcDNA3.1/myc-His(−)B; PD-1, programmed death 1; qPCR, quantitative PCR; TDLN, tumor-draining lymph node; Th, T helper cells; TILs, tumor infiltrating lymphocytes

**ARTICLE HISTORY**
Received 31 October 2016
Revised 30 January 2017
Accepted 1 February 2017

**KEYWORDS**
CD4$^+$ T cell; cytokine; IFN$\gamma$; LYG1; tumor immunotherapy

## Introduction

Cytokines are secreted proteins that play significant roles in antitumor immune responses through regulating the proliferation, activation, differentiation, and survival of lymphocytes.[1] To date, many cytokines have been identified with antitumor function. For example, IL-21 shows antitumor effect in different tumor models by activating T and natural killer (NK) or B cell responses.[2] IL-27, a member of the IL-12 heterodimeric cytokine family, possesses antitumor function against various types of tumors through different mechanisms, such as anti-angiogenesis, antibody-dependent cell-mediated cytotoxicity, direct anti-proliferative effects, or through CD8$^+$ T cells and NK cells.[3]

Many tumors bear tumor-specific antigens or tumor-associated antigens, which make immunotherapy possible through tumor-specific T cells to eliminate tumors.[4] However, tumor-specific immunity is often powerless at tumor sites. One reason is that T cell checkpoints, such as programmed death 1 (PD-1), lead to compromised activation and suppressed functions of tumor-specific T cells.[5] Although the blockade of checkpoint molecules has revolutionized cancer immunotherapy, its effectiveness appears to be limited due to the few numbers of existing tumor-infiltrating T cells. In addition, some tumor types are resistant to checkpoint blockade.[6,7] Another reason is the lack of stimulatory molecules, such as cytokines. The function of tumor-specific T cells depends on the production of cytokines.[1] For example, neutralization of IL-9 in mice accelerated tumor growth, while tumor-specific Th9 cell treatment promoted stronger antitumor responses.[8] T-cell ablation of IL-10 facilitates cancer progression due to the loss of IFN$\gamma$ dependent immune surveillance.[9] Therefore, the identification of novel stimulatory cytokines that have potent antitumor function should have a great value in the improvement of tumor immunotherapy.

To identify novel potential cytokines, our group has established a screening platform using immunomics, including bioinformatics, functional screening, and systematic study, since 2008. Using this strategy, we have identified several novel

**CONTACT** Prof. Wenling Han hanwl@bjmu.edu.cn Department of Immunology, School of Basic Medical Sciences, Peking University Health Science Center, 38 Xueyuan Road, Beijing 100191, China.
Supplemental data for this article can be accessed on the publisher's website.
*These authors contributed equally to this work.

cytokines that have different immune modulatory function.[10-14] LYG1 (lysozyme G-like 1) is one of them. LYG1 belongs to the lysozyme G family. Five types of lysozymes have been identified, of which only the C-type and G-type lysozymes exist in the human genome.[15] The lysozyme G family consists two members, LYG1 and LYG2. In 2011, Huang et al. detected the LYG2 protein in human eye and testis and found that LYG2 recombinant protein inhibited Gram-positive bacterial growth but not Gram-negative bacterial or *Candida albicans* growth.[16] A short communication recently reported that in fish Lyg2 was significantly upregulated in mucosal tissues following bacterial challenge, while Lyg1 showed downregulation.[17] However, the function of LYG1 was unknown.

The lysozyme superfamily has bacteriolytic functions through hydrolyzing ß-1, 4 glycosidic bonds in peptidoglycan and chitin using glycoside hydrolase.[18] Early studies also reported the tumor-inhibiting function of lysozymes. For example, the oral administration of hen egg white lysozyme could significantly reduce the tumor growth and lung metastases of B16 melanoma.[19] Lysozyme expressed by B-16V cells could suppress the tumorigenicity of these cells.[20] Marine lysozyme could inhibit angiogenesis and tumor growth.[21] Egg white lysozyme could increase the number of $CD8^+$ T cells in mice bearing MCa mammary carcinoma.[22]

Based on these clues, in this study, we have verified the secretion of LYG1, investigated the bacteriolytic and tumor-inhibiting function, and explored the mechanism of its antitumor function.

## Results

### *Expression and purification of LYG1*

LYG1 (GeneID: 149999339) was isolated using the immunogenomics strategy described previously.[10] The nucleotide sequence and amino acid sequence data have been submitted to the GenBank databases under accession number NM_174898.2 (Fig. 1A). Human *LYG1* is located on chromosome 2q11.1, encoding 194 amino acids with a lysozyme-like domain (Fig. S1A). To determine the function of LYG1, we first analyzed the expression profile of human LYG1. As shown in Fig. 1B, LYG1 demonstrated the highest expression level in the kidney and lower levels in other tissues.

LYG1 contains a typical signal peptide as predicted by SignalP 4.0 (website). To verify the secretion, LYG1 was overexpressed by transfecting pcDB-LYG1 into HEK293T cells following the BFA blocking assay. As shown in Fig. 1C, the LYG1 protein could be detected at 25 kDa, which is consistent with the predicted molecular mass. The secretion of proteins with N-terminal signal peptides can be blocked by BFA, an inhibitor of the classical (ER–Golgi) secretion pathway.[23] BFA treatment dramatically decreased LYG1 secretion into the supernatant, indicating that LYG1 is a classical secretory protein (Fig. 1C). To examine the signal peptide, eukaryotic LYG1 recombinant protein (rhLYG1) was purified from HEK293T culture supernatants and subjected to N-terminal sequencing. The result (Fig. S1B) showed that the first 19 amino acids constituted the signal peptide of LYG1, in accordance with the prediction by SignalP 4.0.

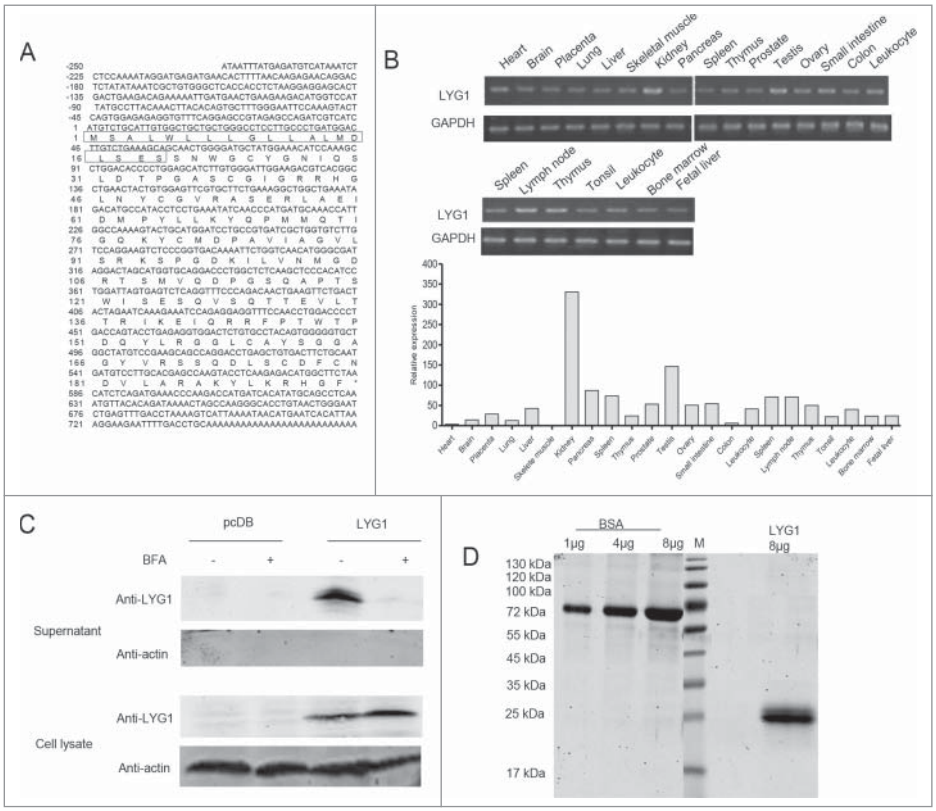


**Figure 1.** Expression and purification of LYG1. (A) Nucleotide sequence and amino acid sequence of human LYG1. The boxes indicate the signal peptide predicted by SignalP 4.0. (B) Expression profile of LYG1 in multiple human tissues and immune cells analyzed by PCR and real-time PCR. (C) Verification of the secretion pathway for LYG1 using the BFA blocking assay. (D) Pure rhLYG1 analysis by SDS-PAGE.

Adequate quantity and quality of rhLYG1 was essential for functional investigation of LYG1. Thus, an efficient transient expression system was established in HEK293F cells by transfection of pcDB-LYG1. Total 15 mg of high-quality rhLYG1 (with a C-terminal Myc-6xhis tag) with high purity (>95%) and low endotoxin (0.125 EU/mg protein) was purified and used in further studies (Fig. 1D).

### *LYG1 showed antitumor activity depending on lymphocytes in vivo*

LYG1 belongs to lysozyme superfamily and contains a lysosome domain. To evaluate the bacteriolytic ability of LYG1, an enzymatic assay that lysed bacteria was performed using *M. lysodeikticus*, which is a typical enzymatic substrate for lysozyme and is generally used to detect bactericidal activity.[24-27] As shown in Fig. S2, rhLYG1 could not lyse *M. lysodeikticus*, while human lysozyme (positive control) exhibited high bacteriolytic activities. The results suggested that LYG1 possessed no bacteriolytic function.

Previous studies have reported that lysozymes exert antitumor activity via different mechanisms, including via the immune system.[19-22] To test whether LYG1 could have antitumor functions, B16 graft melanoma model was adopted. B16 tumor cells were inoculated s.c. into B6 mice, and rhLYG1 (diluted in PBS) or PBS (control) was injected i.p. each day after tumors were established (30–80 $mm^3$). Tumor growth was significantly suppressed upon rhLYG1 treatment in a dose-dependent manner (Fig. 2A and B). In addition, tumor weights (Fig. 2C) and B16 tumor cell numbers (Fig. 2D) also decreased in mice treated with rhLYG1, suggesting that LYG1 might have antitumor effects. Importantly, no apparent adverse effect was observed in the tumor-bearing mice with rhLYG1 treatment, suggesting the safety of using rhLYG1. Similar result was obtained by intra-tumor injection of rhLYG1 (Fig. S3A and B). Given that rhLYG1 itself had no direct effects on B16 cell growth *in vitro* (Fig. 2E), its antitumor effects might involve other mechanisms, such as immune system. Therefore, SCID-beige mice which lack T, B, and NK cells and *Rag1*$^{-/-}$ mice which lack T and B cells were used in B16 graft melanoma

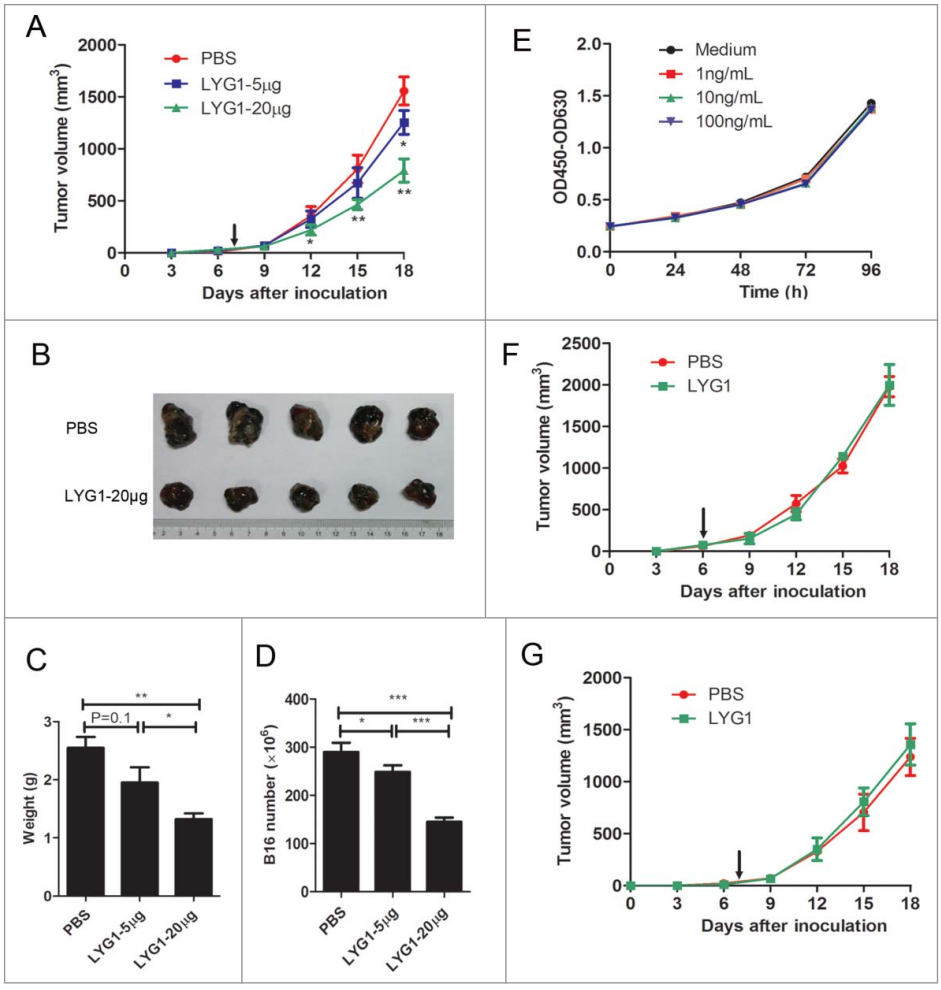


**Figure 2.** Antitumor function of LYG1 is dependent on lymphocytes. (A–D) rhLYG1 inhibited B16 melanoma growth ($n = 6$–8 per group; one representative experiment was shown). B6 mice were inoculated s.c. with $2\times 10^5$ B16 cells in the axilla, and rhLYG1 (5 $\mu$g or 20 $\mu$g) or PBS as a control was injected i.p. every day. Arrows represent the beginning of protein administration. (A) The tumor growth curve. (B) Excised tumors. (C) Tumor weights and (D) B16 cell numbers of excised tumors are shown. (E) CCK-8 assay of B16 cells with or without the addition of the indicated concentration of rhLYG1 *in vitro*. (F–G) B16 tumor progression following treatment with 20 $\mu$g rhLYG1 or PBS in SCID-beige mice (F) ($n = 4$ per group) or in *Rag1*$^{-/-}$ mice (G) ($n = 5$ per group). Arrows represent the beginning of protein administration. Results are representative of three independent experiments and expressed as the mean ± SEM, $^{*}p < 0.05$ and $^{**}p < 0.01$, LYG1–20 $\mu$g (or LYG1–5 $\mu$g) compared with PBS in Fig. 2A, LYG1–20 $\mu$g (or LYG1–5 $\mu$g) compared with PBS and LYG1–20 $\mu$g compared with LYG1–5 $\mu$g in Fig. 2C and D.

model. As shown in Fig. 2F and G, LYG1 failed to inhibit tumor growth in both strains, suggesting that the antitumor effect of LYG1 was dependent on lymphocytes.

### LYG1 antitumor effect was dependent on T cells

To determine the mechanisms of LYG1-mediated tumor inhibition, we first examined tumor-infiltrating lymphocytes (TILs), including $CD4^+$ T, $CD8^+$ T, NK, and B cells, in the tumor-bearing mice treated with 20 $\mu$g rhLYG1 or PBS. As shown in Fig. 3A, the numbers of $CD4^+$ T cells and $CD8^+$ T cells in TILs normalized to the numbers of tumor cells were drastically higher in rhLYG1 group than in PBS-injected controls, showing 3-folds and 2.5-folds, respectively. There was no obvious difference for B and NK cells. Lymphocytes in the tumor draining lymph nodes (TDLNs) and spleens were also measured. In accordance with the TIL results, LYG1 treatment resulted in an increase of $CD4^+$ T cells and $CD8^+$ T cells in both TDLNs and spleens, although a less extent than in TILs. No difference in B and NK cells was observed (Fig. 3B and C). The enrichment of T cells in tumors suggested that LYG1 might promote the expression of chemokines that recruit T cells. Therefore, we examined the expression of seven chemokines (CCL3, CCL4, CCL5, CCL8, CXCL9, CXCL10, and CXCL11) within the tumor under rhLYG1 i.p. injection and intra-tumor injection. In both situations, CCL5, CXCL9, CXCL10, and CXCL11 were upregulated in rhLYG1 group than in PBS group and the increase of CXCL9 was most obviously (Fig. 3D and Fig. S3C). These results indicated LYG1 could increase the expression of some T cell chemokines in tumor microenvironment. To test whether the antitumor effect was dependent on T cells, $CD4^+$ T and $CD8^+$ T cells were depleted using anti-$CD4^+$ and anti-$CD8^+$ monoclonal antibodies (mAbs) separately in the B16 graft melanoma mouse model. The blocking efficiencies using mAbs were greater than 95% (Fig. S4). As illustrated in Fig. 3E and F, the antitumor effect of LYG1 was abrogated after the individual depletion of $CD4^+$ T or $CD8^+$ T cells. Taken together, the above results showed that LYG1 could inhibit B16 tumor growth, and the antitumor effect was dependent on T lymphocytes.

### LYG1 promoted IFN$\gamma$ production by $CD4^+$ T cells

To explore how the antitumor function of LYG1 was mediated by T cells, the effect of LYG1 on the cytokine production

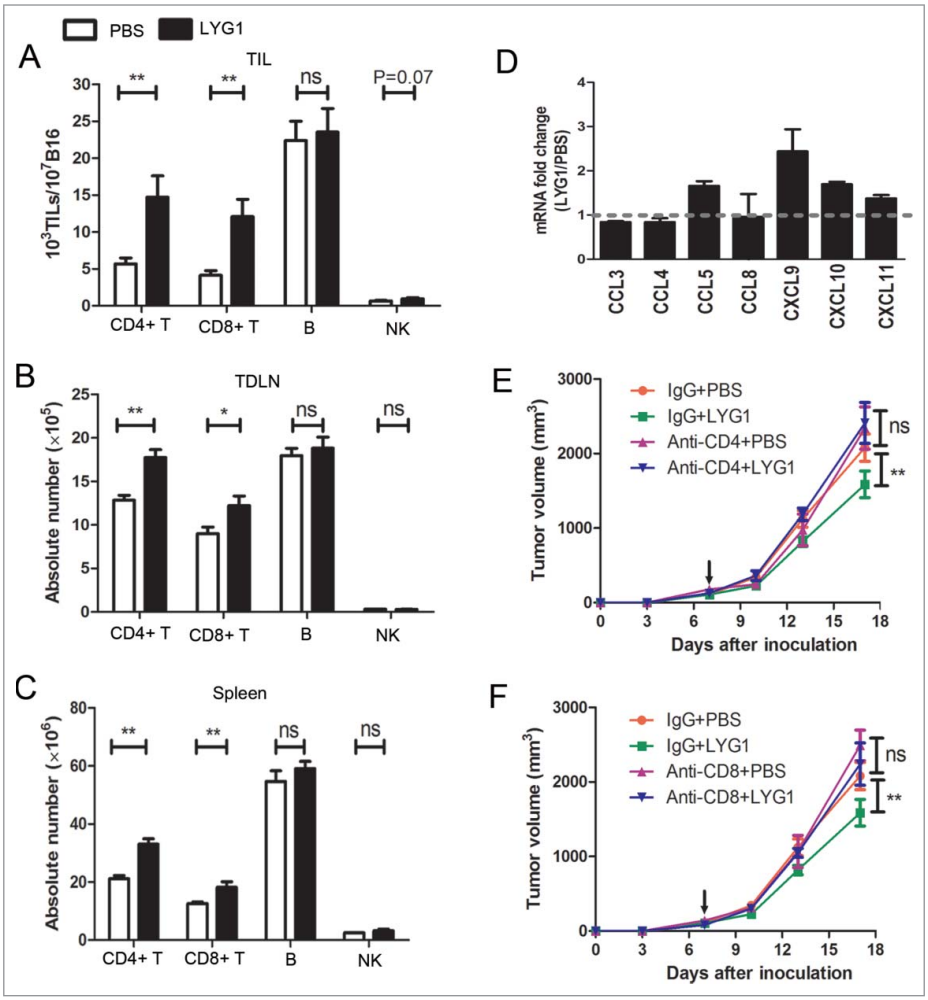


**Figure 3.** T cells mediate the antitumor function of LYG1. (A–C) The absolute numbers of $CD4^+$ T, $CD8^+$ T, B, and NK cells in (A) TILs, (B) TDLNs, and (C) spleens in B16 tumor-bearing mice treated with 20 $\mu$g rhLYG1 or PBS as outlined in Fig. 2A, $n = 6$–8 per group. (D) Chemokines were examined by qPCR in excised tumors, $n = 3$ per group. Data were expressed as ratio of LYG1/PBS. More than one indicated upregulation upon LYG1 injection. (E and F) B16 tumor progression following treatment with 20 $\mu$g LYG1 or PBS and depletion of (E) $CD4^+$ T cells or (F) $CD8^+$ T cells. Arrows represent the beginning of protein administration, $n = 6$–8 per group. Results are representative of three independent experiments and expressed as the mean ± SEM, $^*p < 0.05$ and $^{**}p < 0.01$ compared with PBS.

of T cells was analyzed. First, splenocytes from B6 mice were stimulated with anti-CD3/anti-CD28 mAbs with different concentrations of rhLYG1 (1, 10, and 100 ng/mL) or medium alone (no rhLYG1 protein) added into the culture supernatant. Fig. 4A showed that LYG1 could promote IFN$\gamma$ secretion at a range of low concentrations and the effect fitted a bell-shaped curve with the optimum concentration of 10 ng/mL. As negative controls, Myc-6xhis tag peptide

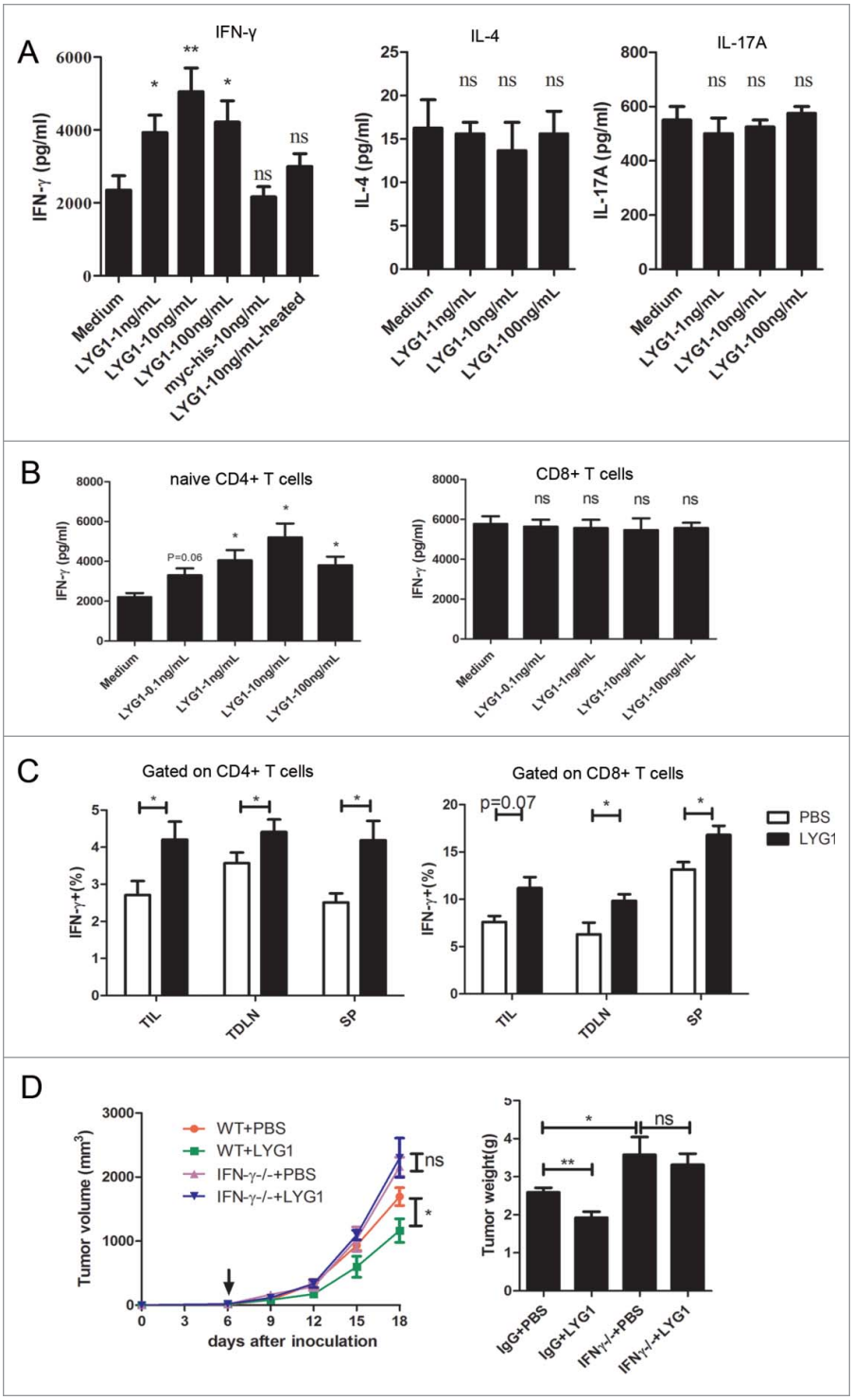


**Figure 4.** LYG1 elicits CD4$^+$ T cell-mediated tumor immunity by promoting IFN$\gamma$ production. (A) IFN$\gamma$, IL-4 and IL-17A production by splenocytes treated with or without different concentrations of rhLYG1 and stimulated with coated anti-CD3 (1 $\mu$g/mL) and soluble anti-CD28 mAbs (0.5 $\mu$g/mL) for 48 h. Medium (LYG1 not added), Myc-6xhis peptide (10 ng/mL) and LYG1-heated (10 ng/mL) were used as negative controls. IFN$\gamma$, IL-4 and IL-17A concentrations in the culture supernatants of cells were measured by ELISA, and the results are shown on the vertical axis. (B) Naive CD4$^+$ T cells or CD8$^+$ T cells were isolated from LNs of WT B6 mice and stimulated with coated anti-CD3 (2 $\mu$g/mL) and soluble anti-CD28 mAbs (1 $\mu$g/mL). Various concentrations of rhLYG1 were added during the process. IFN$\gamma$ concentrations in the culture supernatants of cells were measured by ELISA, and the results are shown on the vertical axis. (C) Single-cell suspensions isolated from TIL, TDLN, and spleen (SP) of tumor-bearing mice treated with 20 $\mu$g LYG1 or PBS were stimulated with PMA and ionomycin for 5 h and then tested for the expression of IFN$\gamma$ by flow cytometry, $n = 6$–8 per group. The percentages of IFN$\gamma^+$ cells gated on CD4$^+$ T cells (left) and CD8$^+$ T cells (right) are shown on the vertical axis. (D) B16 tumor progression and weights in WT and *Ifng*$^{-/-}$ mice treated with 20 $\mu$g LYG1 or PBS, $n = 4$–5 per group. Arrows represent the beginning of protein administration. This panel shows a representative statistical result of three independent experiments. Data are expressed as the mean ± SEM, $^*p < 0.05$ and $^{**}p < 0.01$ compared with medium or PBS.

(Myc-his) or heated LYG1 (LYG1-heated) showed no effects, ruling out the possibility of effect due to the addition of Myc-6xhis tag or the low level of endotoxin in rhLYG1. IL-4 and IL-17A, main cytokines produced by Th2 and Th17 cells, showed no significant changes upon LYG1 stimulation (Fig. 4A). As both $CD4^+$ and $CD8^+$ T cells could produce INF$\gamma$, the effect of LYG1 on naive $CD4^+$ T cells and $CD8^+$ T cells were then evaluated under concentrations of 0.1, 1, 10, and 100 ng/mL. As demonstrated in Fig. 4B, LYG1 remarkably increased IFN$\gamma$ secretion by naïve $CD4^+$ T cells, showing a bell-shaped curve effect with the optimum concentration of 10 ng/mL, similar to the effect on splenocytes (Fig. 4A). However, LYG1 could not enhance IFN$\gamma$ secretion by $CD8^+$ T cells (Fig. 4B). These data highlighted a direct role for LYG1 in promoting IFN$\gamma$ production by $CD4^+$ T cells *in vitro*.

Next, to evaluate the effect of LYG1 on T cells *in vivo*, the expression of IFN$\gamma$ in $CD4^+$ and $CD8^+$ T cells in TILs, TDLNs, and spleens from tumor-bearing mice were tested by flow cytometry. As shown in Fig. 4C, higher percentage of IFN$\gamma^+$ cells were observed in both $CD4^+$ and $CD8^+$ T cells in TILs, TDLNs, and spleens, suggesting the IFN$\gamma$ promoting effect of LYG1 *in vivo*. As LYG1 showed no INF$\gamma$ promoting effect on $CD8^+$ T cell *in*

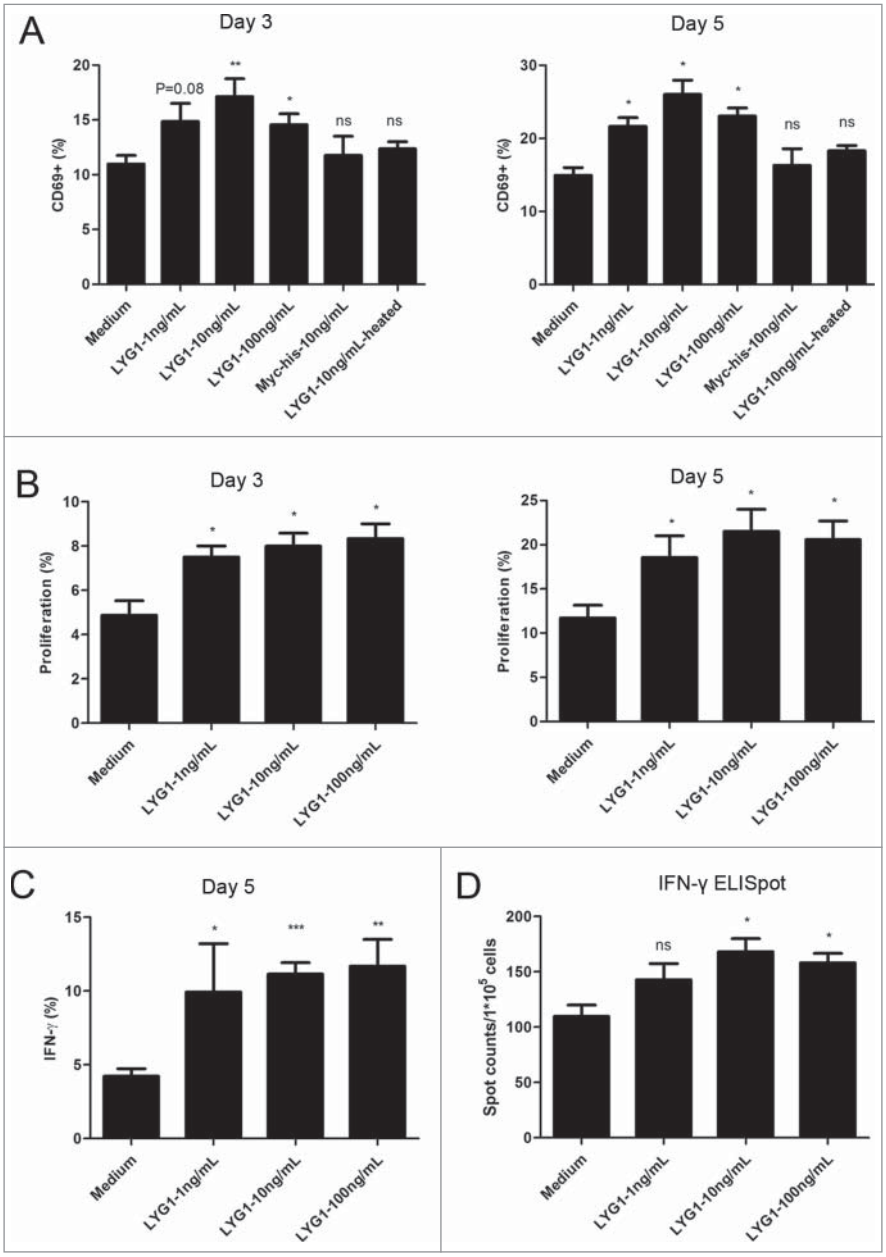


**Figure 5.** LYG1 promotes the activation, expansion, and IFN$\gamma$ production of tumor antigen-specific $CD4^+$ T cells. B6 mice were inoculated s.c. with irradiated B16-OVA cells. After 10 days, the splenocytes were isolated, stimulated with $OVA_{323-339}$ in the presence of rhLYG1 (0, 1, 10, or 100 ng/mL) and then analyzed for activation, proliferation, and IFN$\gamma$ production gated on $CD4^+$ T cells by flow cytometry on day 3 or day 5. (A) The expression of CD69. The frequencies of CD69-expressing cells gated on $CD4^+$ T cells are shown on the vertical axis on day 3 or day 5. (B) Proliferation was determined by the CFSE dilution assay. The percentages of $CD4^+$ T cells that had divided at least once are indicated on day 3 or day 5. (C) The expression of IFN$\gamma$ on day 5. The percentages of IFN$\gamma^+$ cells gated on $CD4^+$ T cells are shown on the vertical axis. (D) Naive $CD4^+$ T cells from OT-II mice were stimulated with irradiated $OVA_{323-339}$-pulsed DCs with the addition of the indicated concentration of rhLYG1. The expression of IFN$\gamma$ at 24 h was measured by ELISPOT. One representative of three independent experiments was shown for each figure. Data are shown as mean ± SEM, $^*p < 0.05$ and $^{**}p < 0.01$ compared with medium (LYG1 not added).

*vitro* (Fig. 4B), the observed promoting effect *in vivo* may due to indirect activation. Further, to investigate whether the effector molecule IFN$\gamma$ was essential for the antitumor function of LYG1, *Ifng*$^{-/-}$ mice were used to establish the B16 graft melanoma model. However, with the deficiency of INF$\gamma$, the antitumor effect of LYG1 was abrogated (Fig. 4D). *Ifng*$^{-/-}$ mice showed larger tumors compared with WT mice (Fig. 4D), which reconfirmed the critical role of IFN$\gamma$ in antitumor immunity. Our data suggested that the antitumor effect of LYG1 was mediated through promoting INF$\gamma$ production by CD4$^+$ T cell.

### *LYG1 promoted the activation, expansion, and IFN$\gamma$ production of tumor antigen-specific CD4$^+$ T cells*

To further explore the antitumor mechanism of LYG1, its effect in the tumor antigen-specific response mediated by CD4$^+$ T cells was evaluated. WT B6 mice were inoculated with irradiated B16-OVA (ovalbumin) cells. The splenocytes were isolated 10 d after inoculation and stimulated with $OVA_{323-339}$, which can stimulate $OVA_{323-339}$-specific CD4$^+$ T cell immune responses, in the presence of rhLYG1 (1, 10, and 100 ng/mL). The activation, expansion, and IFN$\gamma$ production of tumor antigen-specific CD4$^+$ T cells were then examined. Compared with the medium control, LYG1 could increase the expression of CD69, an early activation marker of T cell, from Day 3, and even higher on Day 5, in a bell-shaped curve way (Fig. 5A). LYG1 could also promote the proliferation of tumor antigen-specific CD4$^+$ T cells as determined by dilution of the CFSE signal (Fig. 5B). Furthermore, LYG1 could increase the IFN$\gamma$ production by tumor antigen-specific CD4$^+$ T cells at the indicated three concentrations on Day 5 (Fig. 5C). To test whether LYG1 could directly promote the response of antigen-specific CD4$^+$ T cells without the effects of other lymphocytes, naive CD4$^+$ T cells were isolated from OT-II mice and co-cultured with $OVA_{323-339}$-pulsed DCs in the absence or presence of rhLYG1 (0, 1, 10, and 100 ng/mL). More IFN$\gamma$ producing CD4$^+$ T cells were identified in rhLYG1 stimulation group than in medium control group, as determined by ELISPOT assay (Fig. 5D). This result reinforced that LYG1 could promote antigen-specific response mediated by CD4$^+$ T cells.

### *Lyg1 knockout accelerated tumor growth and inhibited tumor-specific T-cell immune responses*

Conventional *Lyg1* KO mice were constructed to understand the physiologic role of LYG1 in antitumor response (Fig. S5). No obvious changes in the main organs (data not shown), or abnormalities of immune system, including development and cell frequency of T, B, and NK cells, were observed in *Lyg1*$^{-/-}$ mice (Fig. S6). However, when establishing B16 graft melanoma model using *Lyg1*$^{-/-}$ and littermate *Lyg1*$^{+/+}$ mice, *Lyg1* KO mice exhibited accelerated tumor growth (Fig. 6A), reduced numbers of CD4$^+$ T and CD8$^+$ T cells in the TILs, TDLNs, and spleens (Fig. 6B). The KO mice also displayed decreased IFN$\gamma$ producing by T cells (Fig. 6C). In addition to B16 melanomas, the progression of LLC-1 was also tested in *Lyg1*$^{-/-}$ and littermate *Lyg1*$^{+/+}$ mice. Similar results were observed for LLC-1 tumors (Fig. 6D), suggesting that the antitumor effect of LYG1 was not limited to B16 melanomas.

Next, the tumor antigen-specific CD4$^+$ T cell response was examined in B16-OVA tumor-bearing *Lyg1*$^{-/-}$ mice. Fig. 6E and F indicated decreased CD69 expression and INF$\gamma$ production in CD4$^+$ and CD8$^+$ T cells in *Lyg1*$^{-/-}$ mice. Therefore, LYG1 deficiency inhibited the effector functions of tumor-specific T cells.

## Discussion

Using immunogenomics strategy, our group have identified and explored the function of several potential cytokines.[10-14] In this study, we reported LYG1, another molecule identified using the same strategy. We have verified the secretion of LYG1, purified adequate recombinant protein with high quality and explored the function, both *in vitro* and *in vivo*, using rhLYG1 and gene-knockout mice.

LYG1 was a classic secretory protein with the first 19 amino acids as signal peptide. Although LYG1 contains a goose egg white lysozyme (GEWL) domain, it shows almost no bacteriolytic activity on *M. lysodeikticus*. This could be due to the extremely low sequence identity with human lysozymes, although it shares low homology (40%) with LYG2, which was proved to inhibit Gram-positive bacterial growth.[16] Evolutionary immunology studies discovered that the mammalian lysozyme G sequences evolved at an accelerated rate and did not perfectly conserve the known active site catalytic triad of bird enzymes.[28]

Lysozymes have been reported to inhibit tumor growth.[19-22] Therefore, we performed a series of experiments to evaluate the function and mechanisms of antitumor effect of LYG1. We found that rhLYG1 could significantly suppress the growth of B16 tumors in a dose-dependent way. The antitumor effect was mediated by lymphocytes based on the following evidences: (1) no direct inhibition was observed for LYG1 on B16 cells *in vitro*; (2) the antitumor effect was abrogated in SCID-beige mice and *Rag1*$^{-/-}$ mice, both of which lack lymphocytes. We then analyzed how LYG1 affects lymphocytes to exert its antitumor function. TILs often associated with a better outcome in several cancer types, such as melanoma, colorectal cancer, and ovarian cancer.[29] We found that LYG1 treatment could increase the CD4$^+$ T and CD8$^+$ T cells, but not B cells or NK cells, in TILs, TDLNs, and spleens, suggesting that LYG1 seems to exert antitumor function through T cells. This was validated by depleting either CD4$^+$ or CD8$^+$ T cells using mAbs, in which situations the antitumor effect was abrogated, confirming the dependence on both CD4$^+$ and CD8$^+$ T cells. rhLYG1-induced upregulation in the expression of chemokines within tumors is associated with increased T-cell infiltration and antitumor response, which is consistent with the previous studies.[30,31] Our data showed that LYG1 could increase the chemokine secretion in the tumor microenvironment.

Next, we analyzed the effect of LYG1 on CD4$^+$ and CD8$^+$ T cells, *in vitro* and *in vivo*. LYG1 could promote splenocytes to secret IFN$\gamma$, but not IL-4 or IL-17A. Further, we confirmed that LYG1 can only promote CD4$^+$, but not CD8$^+$ T cells, to produce IFN$\gamma$ *in vitro*. Moreover, LYG1 could promote the activation, proliferation, and IFN$\gamma$ production of tumor antigen specific-CD4$^+$ T cells. These data suggested that LYG1

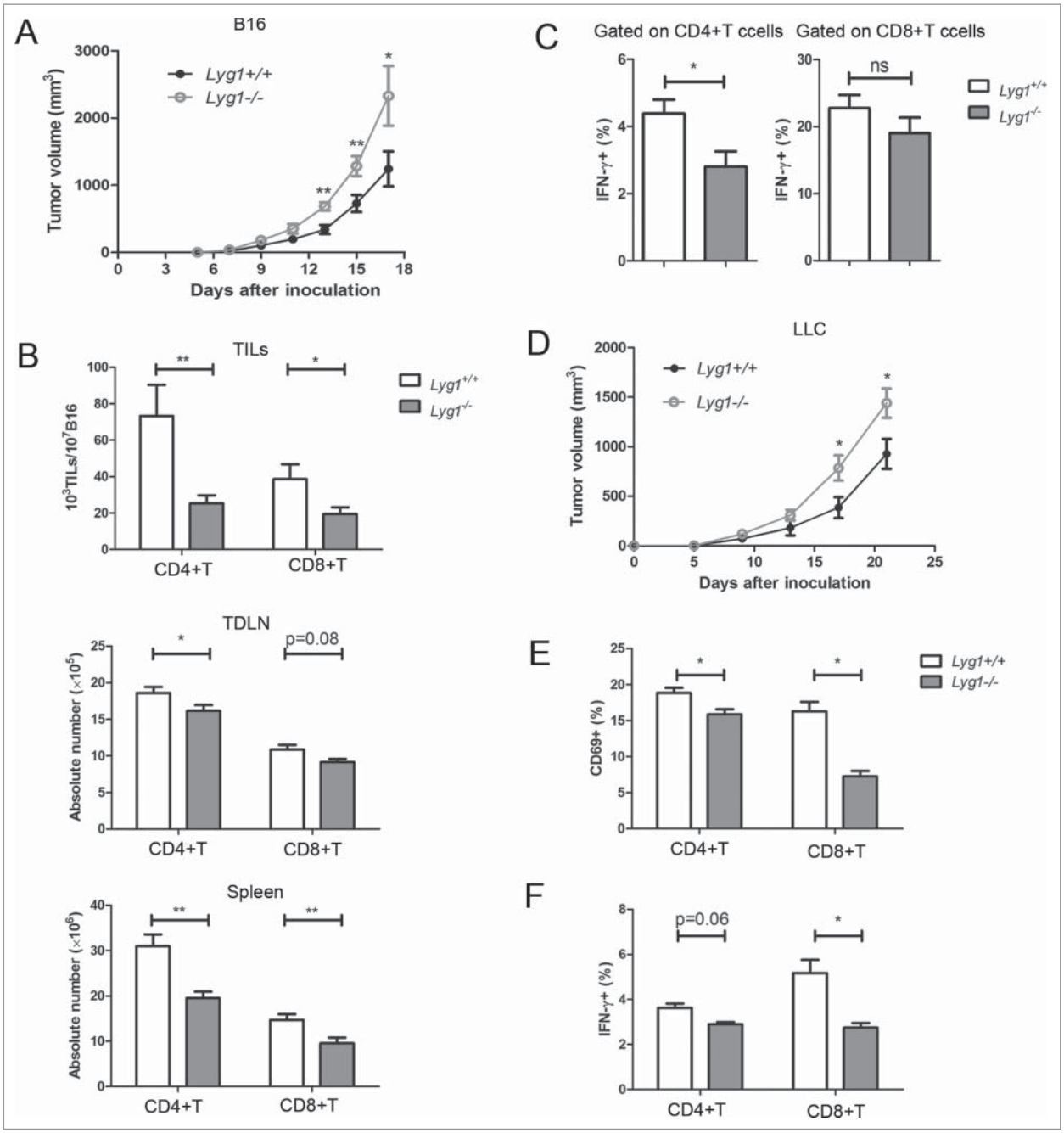


**Figure 6.** *Lyg1* knockout accelerates *in vivo* tumor growth and inhibits tumor-specific T cell immune responses. (A) B16 tumor progression in $Lyg1^{-/-}$ and $Lyg1^{+/+}$ mice. (B) The numbers of $CD4^+$ T and $CD8^+$ T cells in the TILs, TDLNs, and spleens. (C) IFN$\gamma$ production by T cells in the spleens of tumor-bearing mice. $n = 10$–12 per group for A–C. (D) LLC-1 tumor progression in $Lyg1^{-/-}$ and $Lyg1^{+/+}$ mice, $n = 4$–5 per group. (E) The expression of CD69 and (F) IFN$\gamma$ on tumor antigen-specific $CD4^+$ T cells in $Lyg1^{-/-}$ mice and $Lyg1^{+/+}$ mice on day 5 as described methods in Fig. 5, $n = 3$ per group. Data are expressed as the mean ± SEM, $^*p < 0.05$ and $^{**}p < 0.01$ compared with $Lyg1^{+/+}$ mice.

possessed direct promoting effects on $CD4^+$ T cells. However, *in vivo* experiments showed that in addition to $CD4^+$ T cells, LYG1 could also promote $CD8^+$ T cells to produce IFN$\gamma$. This may due to the priming effect of $CD4^+$ T cells, which could augment tumor-specific $CD8^+$ T cell responses via cytokine production, such as IL-2 and IFN$\gamma$.[32,33] This could also explain why the antitumor effect of LYG1 was also dependent on $CD8^+$ T cells. It seemed that two steps happened in LYG1 mediated antitumor functions. First, LYG1 promoted the tumor antigen-specific $CD4^+$ T cells to proliferate and produce large amount of IFN$\gamma$, which in turn enhanced the tumor-killing function of $CD8^+$ T cells and thus inhibited the tumor growth.

In the whole process, IFN$\gamma$ seems to be the key effector molecule in antitumor response. This was confirmed by the abrogation of antitumor effect of LYG1 in $Ifng^{-/-}$ mice. IFN$\gamma$ plays an essential role in regulating T cell-mediated tumor immune responses. It can up-regulate MHC molecules on tumor cells, increase T cell recognition, enhance cytotoxicity of $CD8^+$ T cells and suppress tumor angiogenesis.[32,34] Our data also reinforced the critical antitumor effect of IFN$\gamma$, as $Ifng^{-/-}$ mice showed severe tumor progression and tumor weight than WT mice.

Furthermore, we used *Lyg1*$^{-/-}$ mice to validate the tumor-inhibiting effect of LYG1. *Lyg1*$^{-/-}$ mice showed accelerated tumor growth than WT mice, this may be due to the decreased T cell number in TILs, TDLNs, and spleens, and the deficiency of INF$\gamma$ production by T cells. The tumor-inhibiting effect of LYG1 may be effective on different cancer types, as we found the deficiency of LYG1 could result in accelerated LLC1 tumor growth, which is a Lewis lung carcinoma cell line.

LYG1 possesses some basic features of cytokines, such as follows: (1) it is a classical secreted protein with a typical signal peptide; (2) it has a small molecule size with only 175 amino acids in the mature protein; and (3) it shows immune-regulatory effects at a range of low concentrations exhibiting a bell-shaped curve. Cytokines exert functions through binding to their specific receptors.[12] However, the receptor of LYG1 has not yet been identified. In summary, our study identified LYG1 as a novel secretory protein showing some cytokine features. It could inhibit tumor growth through promoting the activation, proliferation, and function of CD4$^+$ T cells without safety issues, offering a potential implication for tumor therapy.

## Materials and methods

### Mice

Six- to eight-week-old female C57BL/6 (B6) and SCID-beige mice were purchased from Vital River Laboratories. *Ifng*$^{-/-}$ mice (B6.129S7-IFN$\gamma$tm1Ts/J) were purchased from the Model Animal Research Center of Nanjing University. *Rag1*$^{-/-}$ (B6 background) mice and OT-II mice ($OVA_{323-339}$ peptide-specific CD4$^+$ TCR transgenic mice, B6 background) were generous gifts from Dr. Qing Ge (Peking University, Beijing, China). The Lyg1 conventional knockout mice were generated by the RIKEN Yokohama Institute (Yokohama, Japan). Homozygous knockout (KO) or transgenic mice and the littermate wild-type (WT) mice were used for all related experiments. All mice were bred in the animal breeding facilities at Peking University Health Science Center under specific pathogen-free conditions, and all studies were approved by the Ethics Committee of Peking University Health Science Center.

### Cell culture

B16 cells, B16-OVA cells (an OVA-transfected clone derived from the murine melanoma cell line B16,[35] a kind gift from Jing Huang, Peking University), HEK293T cells, and Lewis lung carcinoma cells (LLC1) were obtained from our collaborators and maintained in DMEM (Gibco, 8116167) supplemented with 10% FBS (Hyclone, SH30084.03). All lymphocytes and splenocytes were cultured in RPMI 1640 medium (Gibco, 8116163) supplemented with 10% heat-inactivated FBS. All cells were grown at 37 °C in a humidified incubator containing 5% $CO_2$.

### Vector construction

The open reading frame of LYG1 was amplified using human spleen and fetal liver mixed cDNA libraries (Clontech, Cat. No. 636743 and 636748) as templates with the forward primer 5′–GCGGCCGCCACCATGTCTGCATTGTGGCTGCTGC–3′ and the reverse primer 5′–GGTACCGCGAAGCCATGTCTCTT-GAGGTACTTG–3′. The amplification were purified and subcloned into pcDNA3.1/myc-His(−)B (Invitrogen, V855–20) after digestion with *Not*I and *Kpn*I (named pcDB-LYG1).

### Expression profile by PCR and real-time PCR

The human multiple tissue cDNA libraries and immune system tissue cDNA library were purchased from Clontech. Nested PCR was performed to test the expression profile of LYG1 with the following primers: the external forward primer: 5′–TTTCAGGAGCCGTAGAGCC–3′; the external reverse primer: 5′–TGATCATGGTCTTGGGTTT–3′; the internal primers were the same pair used in vector construction. Quantitative PCR (qPCR) was performed using primers of 5′–CCTGCCGTGATCGCTG–3′ and 5′–ACTAC-TAGAATCAAA–3′ on ABI PRISM 7000 Sequence Detection System (Applied Biosystems). All samples were normalized against GAPDH using the comparative Ct method (ddCt).

### Secretion verification, expression, and purification of LYG1

LYG1 was overexpressed in HEK293T cells via transfection of pcDB-LYG1. BFA block assay was performed as described previously.[10] Supernatant and cell lysate were examined by Western blot. The rabbit anti-LYG1 polyclonal antibody (1 $\mu$g/mL) generated in house and HRP-conjugated goat anti-rabbit IgG (1:5,000 dilution, Cell Signaling Technology, 7074) were used as the primary and secondary antibody, respectively. An efficient transient expression system was established in HEK293F cells as described previously method (with its native signal peptide) to obtain sufficient recombinant protein with high-quality.[36] Supernatants were collected and purified by affinity chromatography using Ni-Sepharose 6 Fast Flow column (GE Healthcare, 11–0008). SDS-PAGE followed by Coomassie brilliant blue staining was conducted to assess the purity of rhLYG1 protein. BCA protein assay (Pierce, 23225) was performed to measure the concentration. BioWhittaker Limulus Amebocyte Lysate QCL$^-$1000 pyrogen testing (LONZA, 50–648U) was used to detect the endotoxin level of purified rhLYG1 protein.

### Bacteriolytic assay

*Micrococcus lysodeikticus* (*M. lysodeikticus*) bacterial cell was purchased from Sigma (M0508). 0.015% lyophilized *M. lysodeikticus* suspension in 66 mM potassium phosphate buffer, pH 6.24 (buffer A) was prepared at 25 °C to obtain a constant absorbance between 0.7 and 0.8 at 450 nm. Different final concentrations of LYG1 or human lysozyme (Sigma, L6876) were prepared in cold buffer A and were added into the cuvettes containing the bacterial suspension. The absorbance at 450 nm was measured after 5 min reaction. The decrease in absorbance at 450 nm indicated bacteriolytic activity against *M. lysodeikticus*.

### Cell proliferation assay

Cell proliferation was analyzed using the Cell Counting Kit-8 (CCK-8, Dojindo Laboratories, CK04). The B16 cells were seeded in 96-well plates at a density of 3,000 cells/100 $\mu$L per well in triplicate and incubated with different concentrations of rhLYG1 (0, 1, 10, and 100 ng/mL). 10 $\mu$L CCK-8 solution was added into each well at indicated time point. After 2 h, 450nm and 630 nm absorbance were measured.

### Graft tumor models

For B16 melanoma model, mice were inoculated subcutaneously (s.c.) with $2 \times 10^5$ B16 cells in the axilla (day 0). Tumors were measured along two orthogonal axes (a = length, b = width) and tumor volume was calculated by the formula: volume = $a \times b^2/2$. rhLYG1 or PBS was injected intraperitoneally (i.p.) every day or intra-tumor every other day after tumors were established (tumor volume 30–80 $mm^3$, approximately 6–8 d). Tumors were excised and weighed. TILs were isolated using Percoll (GE Healthcare, 17–0891) and tested for different lymphocyte populations by flow cytometry. The numbers of lymphocytes were normalized to the numbers of tumor cells (per $10^7$). mRNA was extracted from excised tumors and chemokines were examined by qPCR (Primers in Table 1).

For Lewis lung carcinoma model, mice were injected s.c. with $1 \times 10^6$ LLC1 cells in the axilla. Tumor volumes and weights were measured using the same method described above.

### In vivo depletion of $CD4^+$ and $CD8^+$ T cell

Mice were injected i.p. with 0.5 mg rat anti-$CD8^+$ (clone 2.43) or anti-$CD4^+$ (clone GK1.5) mAbs or rat IgG (Beijing Zsbio. Co., ZDR-5008) in 200 $\mu$L PBS on day 1 before injection of rhLYG1. Antibodies were injected every 3 d afterward to maintain the depletion. The depletion of $CD4^+$ and $CD8^+$ T cells were consistently greater than 95% as determined by flow cytometry. The anti-$CD8^+$ and anti-$CD4^+$ mAbs were kindly provided by Dr Xiaoyan Qiu (Peking University, Beijing, China).

### Activation, expansion of mouse T cells

$CD4^+$ T cells, $CD8^+$ T cells, or naive $CD4^+$ T cells ($CD4^+CD62L^{high}CD25^-CD44^{low}$) were sorted from the LNs of mice by FACSAria cell sorter (BD Biosciences). The sorted T cells or splenocytes were cultured in 48-well plates ($5 \times 10^5$/500 $\mu$L) coated with 2 $\mu$g/mL (or 1 $\mu$g/mL) anti-mouse CD3e (BD Biosciences, 553057) in the presence of 1 $\mu$g/mL (or 0.5 $\mu$g/mL) soluble anti-mouse CD28 (BD Biosciences, 553294) and different concentrations of rhLYG1 (0, 1, 10, and 100 ng/mL) for 48 h.

For *in vitro* activation of tumor antigen-specific T cells, B6 mice were injected with $1 \times 10^6$ 200 Gy-irradiated B16-OVA cells s.c. in the axilla. After 10 days, splenocytes were obtained and stimulated with 1 $\mu$g/mL $OVA_{323-339}$ peptide (Chinese Peptide Company, Hangzhou, MISC-011B) with or without different concentrations of rhLYG1 for 3 or 5 d. CD69 and IFN$\gamma$ expression was analyzed by flow cytometry. For proliferation assay, splenocytes were labeled with CFSE (Invitrogen, C34554) and stimulated with 1 $\mu$g/mL $OVA_{323-339}$ peptide in the presence of different concentrations of rhLYG1 (0, 1, 10, and 100 ng/mL) and then detected by flow cytometry.

For antigen-specific stimulation of naive $CD4^+$ T cells from OT-II mice, dendritic cells (DCs) were first prepared. Spleens from WT B6 mice were cut into pieces, and treated with 2 mg/mL collagenase (Roche, 11088858001) and 20 U/mL DNase I (Sigma, D4263) for 90 min with 10 mM EDTA added for the last 10 min. The whole process was under 250 rpm centrifugation at 37 °C. Interface cells containing DCs were recovered by using Ficoll/Hypaque density gradient centrifugation at 2,500 rpm for 20 min and subjected to cell sorting to obtain $CD11c^+$ DCs. DCs were then pulsed with 1 $\mu$g/mL $OVA_{323-339}$ overnight and irradiated at 30 Gy and then cocultured with naive $CD4^+$ T cells sorted from LNs of OT-II mice (DC:T = 1:10) with different concentrations of rhLYG1 (0, 1, 10, and 100ng/mL) for 24 h. IFN$\gamma$ producing cells were detected by ELISPOT (Dakewe Biotech Co., Ltd., DKW22–2000–096s).

### Flow cytometry, antibodies, and ELISA

Flow cytometry was performed using the following anti-mouse antibodies: PE-Cy7-CD45 (eBioscience, 25–0451), PerCP-Cy5.5-$CD4^+$ (BD Biosciences, 553052), FITC-$CD8^+$ (eBioscience, 11–0081), PE-NK1.1 (eBioscience, 12–5941), APC-B220 (Biolegend, 103212), FITC-CD11c (eBioscience, 11–0114), FITC-CD44 (eBioscience, 11–0441), PE-CD62L (Biolegend, 104408), APC-CD25 (eBioscience, 17–0251), PE-CD69 (eBioscience, 12–0691), and APC-IFN$\gamma$ (Biolegend, 505810). Single-cell suspensions prepared from the spleen, lymph node (LN), thymus, bone marrow, or TILs were kept on ice and blocked by incubation with anti-Fc receptor antibody in PBS. For membrane molecule analysis, cells were labeled with fluorescent conjugated antibodies at 4 °C for 30 min followed by two washes with cold PBS. For cytokine analysis, cells were stimulated *ex vivo* with 50 ng/mL PMA (Sigma, P1585) and 500 ng/mL ionomycin (Sigma, I3909) in the presence of GolgiStop (BD Biosciences, 554724) for 5 h before cells were harvested for analysis. Cells were first stained with surface markers and then fixed and permeabilized with Cytofix/Cytoperm kit (BD Biosciences, 554714) according to the manufacturer's instructions for intracellular staining. Flow cytometry analysis was performed on FACSVerse or FACSCalibur flow cytometer (BD Biosciences) and analyzed with FlowJo software. IFN$\gamma$, IL-4, and IL-17A in supernatants

**Table 1.** Primers used in qPCR to examine mouse chemokines. qPCR was performed for quantitative analyses in an ABI Prism 7000 Sequence Detection System (Applied Biosystems). Amplifications were performed using Universal Probe Library (UPL) probes. The quantification data were analyzed with ABI Prism 7000 SDS software. The expression levels of the target genes were normalized to the internal standard gene GAPDH.

| Chemokine | Primers-forward (5′–3′) | Primers-reverse (5′–3′) |
|---|---|---|
| CCL3 | CCATGACACTCTGCAACCAA | GTGGAATCTTCCGGCTGTAG |
| CCL4 | GCCCTCTCTCTCCTCTTGCT | GGAGGGTCAGAGCCCATT |
| CCL5 | TGCAGAGGACTCTGAGACAGC | GAGTGGTGTCCGAGCCATA |
| CCL8 | TTCTTTGCCTGCTGCTCATA | GCAGGTGACTGGAGCCTTAT |
| CXCL9 | CTTTTCCTCTTGGGCATCAT | GCATCGTGCATTCCTTATCA |
| CXCL10 | GCTGCCGTCATTTTCTGC | TCTCACTGGCCCGTCATC |
| CXCL11 | TGCTGAGATGAACAGGAAGGT | CGCCCCTGTTTGAACATAAG |
| GAPDH | CACCAACTGCTTAGCCCCC | TCTTCTGGGTGGCAGTGATG |

were measured by ELISA (eBioscience, Ready-Set-Go! 88–7314, 88–7044 and 88–7371) according to the manufacturer's instructions.

### *Statistical analysis*

The data are expressed as the mean ± SEM and tested for statistical significance with Student's t-test using GraphPad Prism 5 software. $^{*}p < 0.05$, $^{**}p < 0.01$, and $^{***}p < 0.001$.

## Disclosure of potential conflicts of interest

No potential conflicts of interest were disclosed.

## Acknowledgments

The authors would like to thank Prof. Dalong Ma for insightful suggestions at Peking University Health Science Center (Beijing, China) and Prof. Jiyang Wang at the RIKEN Yokohama Institute (Yokohama, Japan) for constructing *Lyg1*$^{-/-}$ mice.

## Funding

This work was supported by the National Natural Science Foundation of China (31270948) and the Program for Innovation of New Drugs (2013ZX09103003–023).

## References

1. Pulliam SR, Uzhachenko RV, Adunyah SE, Shanker A. Common gamma chain cytokines in combinatorial immune strategies against cancer. Immunol Lett 2016; 169:61-72; PMID:26597610; http://dx.doi.org/10.1016/j.imlet.2015.11.007
2. Croce M, Rigo V, Ferrini S. IL-21: a pleiotropic cytokine with potential applications in oncology. J Immunol Res 2015; 2015:696578; PMID:25961061; http://dx.doi.org/10.1155/2015/696578
3. Yoshimoto T, Chiba Y, Furusawa J, Xu M, Tsunoda R, Higuchi K, Mizoguchi I. Potential clinical application of interleukin-27 as an antitumor agent. Cancer Sci 2015; 106:1103-10; PMID:26132605; http://dx.doi.org/10.1111/cas.12731
4. Blankenstein T, Coulie PG, Gilboa E, Jaffee EM. The determinants of tumour immunogenicity. Nat Rev Cancer 2012; 12:307-13; PMID:22378190; http://dx.doi.org/10.1038/nrc3246
5. Pardoll DM. The blockade of immune checkpoints in cancer immunotherapy. Nat Rev Cancer 2012; 12:252-64; PMID:22437870; http://dx.doi.org/10.1038/nrc3239
6. Shin DS, Ribas A. The evolution of checkpoint blockade as a cancer therapy: what's here, what's next? Curr Opin Immunol 2015; 33:23-35; PMID:25621841; http://dx.doi.org/10.1016/j.coi.2015.01.006
7. Restifo NP, Smyth MJ, Snyder A. Acquired resistance to immunotherapy and future challenges. Nat Rev Cancer 2016; 16:121-6; PMID:26822578; http://dx.doi.org/10.1038/nrc.2016.2
8. Lu Y, Hong S, Li H, Park J, Hong B, Wang L, Zheng Y, Liu Z, Xu J, He J et al. Th9 cells promote antitumor immune responses *in vivo*. J Clin Invest 2012; 122:4160-71; PMID:23064366; http://dx.doi.org/10.1172/JCI65459
9. Dennis KL, Saadalla A, Blatner NR, Wang S, Venkateswaran V, Gounari F, Cheroutre H, Weaver CT, Roers A, Egilmez NK et al. T-cell expression of IL10 is essential for tumor immune surveillance in the small intestine. Cancer Immunol Res 2015; 3:806-14; PMID:25855122; http://dx.doi.org/10.1158/2326-6066.CIR-14-0169
10. Guo X, Zhang Y, Wang P, Li T, Fu W, Mo X, Shi T, Zhang Z, Chen Y, Ma D et al. VSTM1-v2, a novel soluble glycoprotein, promotes the differentiation and activation of Th17 cells. Cell Immunol 2012; 278:136-42; PMID:22960280; http://dx.doi.org/10.1016/j.cellimm.2012.07.009
11. Pan W, Cheng Y, Zhang H, Liu B, Mo X, Li T, Li L, Cheng X, Zhang L, Ji J et al. CSBF/C10orf99, a novel potential cytokine, inhibits colon cancer cell growth through inducing G1 arrest. Sci Rep 2014; 4:6812; PMID:25351403; http://dx.doi.org/10.1038/srep06812
12. Wang W, Li T, Wang X, Yuan W, Cheng Y, Zhang H, Xu E, Zhang Y, Shi S, Ma D et al. FAM19A4 is a novel cytokine ligand of formyl peptide receptor 1 (FPR1) and is able to promote the migration and phagocytosis of macrophages. Cell Mol Immunol 2015; 12:615-24; PMID:25109685; http://dx.doi.org/10.1038/cmi.2014.61
13. Fu W, Cheng Y, Zhang Y, Mo X, Li T, Liu Y, Wang P, Pan W, Chen Y, Xue Y et al. The secreted form of transmembrane protein 98 promotes the differentiation of T Helper 1 cells. J Interferon Cytokine Res 2015; 35:720-33; PMID:25946230; http://dx.doi.org/10.1089/jir.2014.0110
14. Wang X, Li T, Wang W, Yuan W, Liu H, Cheng Y, Wang P, Zhang Y, Han W. Cytokine-like 1 chemoattracts monocytes/macrophages via CCR2. J Immunol 2016; 196:4090-9; PMID:27084102; http://dx.doi.org/10.4049/jimmunol.1501908
15. Robertus JD, Monzingo AF, Marcotte EM, Hart PJ. Structural analysis shows five glycohydrolase families diverged from a common ancestor. J Exp Zool 1998; 282:127-32; PMID:9723170; http://dx.doi.org/10.1002/(SICI)1097-010X(199809/10)282:1/2%3c127::AID-JEZ14%3e3.0.CO;2-R
16. Huang P, Li WS, Xie J, Yang XM, Jiang DK, Jiang S, Yu L. Characterization and expression of HLysG2, a basic goose-type lysozyme from the human eye and testis. Mol Immunol 2011; 48:524-31; PMID:21093056; http://dx.doi.org/10.1016/j.molimm.2010.10.008
17. Gao C, Fu Q, Zhou S, Song L, Ren Y, Dong X, Su B, Li C. The mucosal expression signatures of g-type lysozyme in turbot (Scophthalmus maximus) following bacterial challenge. Fish Shellfish Immunol 2016; 54:612-9; PMID:27189917; http://dx.doi.org/10.1016/j.fsi.2016.05.015
18. Mandal A, Klotz KL, Shetty J, Jayes FL, Wolkowicz MJ, Bolling LC, Coonrod SA, Black MB, Diekman AB, Haystead TA et al. SLLP1, a unique, intra-acrosomal, non-bacteriolytic, c lysozyme-like protein of human spermatozoa. Biol of Reprod 2003; 68:1525-37; PMID:12606493; http://dx.doi.org/10.1095/biolreprod.102.010108
19. Sava G. Reduction of B16 melanoma metastases by oral administration of egg-white lysozyme. Cancer Chemother Pharmacol 1989; 25:221-2; PMID:2598413; http://dx.doi.org/10.1007/BF00689588
20. Guzel AI, Kasap H, Tuncer I, Ozgunen K, Sertdemir Y, Kasap M, Ozcan N, Yilmaz MB, Pazarbasi A. Suppression of the tumorigenicity of B-16V melanoma cells via lysozyme gene. Cancer Biother Radiopharm 2008; 23:603-8; PMID:18999932; http://dx.doi.org/10.1089/cbr.2008.0516
21. Ye J, Wang C, Chen X, Guo S, Sun M. Marine lysozyme from a marine bacterium that inhibits angiogenesis and tumor growth. Appl Microbiol Biotechnol 2008; 77:1261-7; PMID:18043915; http://dx.doi.org/10.1007/s00253-007-1269-1
22. Pacor S, Giacomello E, Bergamo A, Gagliardi R, Cocchietto M, Sava G. Cytofluorimetric analysis of gut-intraepithelial and mesenteric lymph node lymphocytes of tumour bearing mice fed with egg-white lysozyme. Anticancer Res 1996; 16:145-9; PMID:8615600
23. Miller SG, Carnell L, Moore HH. Post-Golgi membrane traffic: brefeldin A inhibits export from distal Golgi compartments to the cell surface but not recycling. J Cell Biol 1992; 118:267-83; PMID:1629235; http://dx.doi.org/10.1083/jcb.118.2.267
24. Abouhmad A, Mamo G, Dishisha T, Amin MA, Hatti-Kaul R. T4 lysozyme fused with cellulose binding module for antimicrobial cellulosic wound dressing materials. J Appl Microbiol 2016; 121(1):115-25; PMID:27028513; http://dx.doi.org/10.1111/jam.13146
25. Zheng L, Wan Y, Yu L, Zhang D. Lysozyme as a recognition element for monitoring of bacterial population. Talanta 2016; 146:299-302; PMID:26695267; http://dx.doi.org/10.1016/j.talanta.2015.08.056
26. Vasilescu A, Gaspar S, Gheorghiu M, David S, Dinca V, Peteu S, Wang Q, Li M, Boukherroub R, Szunerits S. Surface Plasmon Resonance based sensing of lysozyme in serum on Micrococcus lysodeikticus-modified graphene oxide surfaces. Biosens Bioelectron 2016; 89 (Pt 1):525-31; PMID:27037159; http://dx.doi.org/10.1016/j.bios.2016.03.040
27. Rossi B, Campia P, Merlini L, Brasca M, Pastori N, Farris S, Melone L, Punta C, Galante YM. An aerogel obtained from chemo-enzymatically

oxidized fenugreek galactomannans as a versatile delivery system. Carbohydr Polym 2016; 144:353-61; PMID:27083827; http://dx.doi.org/10.1016/j.carbpol.2016.02.007
28. Irwin DM. Evolution of the vertebrate goose-type lysozyme gene family. BMC Evol Biol 2014; 14:188; PMID:25167808; http://dx.doi.org/10.1186/s12862-014-0188-x
29. Fridman WH, Pages F, Sautes-Fridman C, Galon J. The immune contexture in human tumours: impact on clinical outcome. Nat Rev Cancer 2012; 12:298-306; PMID:22419253; http://dx.doi.org/10.1038/nrc3245
30. Harlin H, Meng Y, Peterson AC, Zha Y, Tretiakova M, Slingluff C, McKee M, Gajewski TF. Chemokine expression in melanoma metastases associated with CD8+ T-cell recruitment. Cancer Res 2009; 69:3077-85; PMID:19293190; http://dx.doi.org/10.1158/0008-5472.CAN-08-2281
31. Geng D, Kaczanowska S, Tsai A, Younger K, Ochoa A, Rapoport AP, Ostrand-Rosenberg S, Davila E. TLR5 ligand-secreting T cells reshape the tumor microenvironment and enhance antitumor activity. Cancer Res 2015; 75:1959-71; PMID:25795705; http://dx.doi.org/10.1158/0008-5472.CAN-14-2467
32. Kennedy R, Celis E. Multiple roles for CD4+ T cells in anti-tumor immune responses. Immunol Rev 2008; 222:129-44; PMID:18363998; http://dx.doi.org/10.1111/j.1600-065X.2008.00616.x
33. Keene JA, Forman J. Helper activity is required for the *in vivo* generation of cytotoxic T lymphocytes. J Exp Med 1982; 155:768-82; PMID:6801178; http://dx.doi.org/10.1084/jem.155.3.768
34. Capobianchi MR, Uleri E, Caglioti C, Dolei A. Type I IFN family members: similarity, differences and interaction. Cytokine Growth Factor Rev 2015; 26:103-11; PMID:25466633; http://dx.doi.org/10.1016/j.cytogfr.2014.10.011
35. Merad M, Sugie T, Engleman EG, Fong L. *In vivo* manipulation of dendritic cells to induce therapeutic immunity. Blood 2002; 99:1676-82; PMID:11861283; http://dx.doi.org/10.1182/blood.V99.5.1676
36. Liu H, Zou X, Li T, Wang X, Yuan W, Chen Y, Han W. Enhanced production of secretory glycoprotein VSTM1-v2 with mouse IgGkappa signal peptide in optimized HEK293F transient transfection. J Biosci Bioeng 2016; 121:133-9; PMID:26140918; http://dx.doi.org/10.1016/j.jbiosc.2015.05.016